HYDROLOGICAL PROCESSES, VOL. 10, 1329–1343 (1996)

INCORPORATING RADIATION INPUTS INTO THE SNOWMELT RUNOFF MODEL

KAYE BRUBAKER, ALBERT RANGO AND WILLIAM KUSTAS

USDA Hydrology Laboratory, Beltsville, MD 20705, USA

ABSTRACT

Process-based, distributed-area snowmelt runoff models operating at small scales are essential to understand subtle effects of climate change, but require data not commonly available. Temperature index models operating over large areas provide realistic simulations of basin runoff with operationally available data, but lack rigorous physically based algorithms. A compromise between the two types of models is required to provide realistic evaluations of basin response to environmental changes in cold regions. One adaptation that is uniformly required for snowmelt models is the use of remotely sensed data, either as input or in model validation. At a minimum, snowmelt forecasting models need to incorporate snowcover extent information, which is currently obtained operationally. As more remote sensing capabilities come on line, models should accept upgraded information on snow water equivalent; additional remotely sensed information on landcover, frozen soil, soil moisture, cloudiness and albedo would also be useful.

Adaptations to the semi-distributed snowmelt runoff model (SRM) are underway to make it more physically based for use in large area studies. A net radiation index has been added to the model, which formerly used only a temperature (degree–day) index to melt snow from a basin's elevation zones. The addition of radiation to the SRM allows the basin to be subdivided into hydrological response units by general aspect (orientation) as well as elevation. Testing of the new radiation-based SRM with measured radiation from a small research basin is the first step towards large scale simulations. Results from the W-3 research basin in Vermont, USA are promising. In the radiation version, the factor that multiplies the degree–day index is estimated independently of model output and is held constant throughout the season, in contrast with the degree–day version, where the corresponding factor is allowed to increase throughout the season. Without calibrating or optimizing on this important parameter, the goodness-of-fit measure R^2 is improved in two out of six test years when the radiation version of the SRM is used in place of the degree–day version in melt season simulations. When the accumulation of error is eliminated with periodic updating of streamflow, more significant improvement is noted with radiation included.

KEY WORDS snowmelt; runoff; degree–day; net radiation

INTRODUCTION

Process-based, distributed-area snowmelt runoff models are essential for understanding snow hydrology processes and evaluating subtle effects of climate change. However, such models operate best in restricted areas or in small basins; when applied to large basins, they require enormous amounts of input data and necessitate the estimation of many model parameters. Temperature index models operating over large areas and basins provide realistic simulations of discharge while requiring more manageable amounts of input data. A compromise between the two types of models is required to provide realistic, process-based evaluations of large-basin runoff response to environmental changes in cold regions, e.g. climate change. One possible solution is the use of physically based, data-intensive models over very small sub-basins (where the data requirements are not overwhelming) and the use of the less data intensive, temperature index models over large basins.

Another approach is to combine the two types of models, i.e. make the degree–day approach for a snowmelt runoff model more physically based by adding a radiation-based snowmelt component, while making the model more distributed with the addition of hydrological response units (HRUs) based on aspect

0885–6087/96/101329–15

Accepted 10 April 1996

classes as well as elevation zones. Such an approach would permit model use over large areas, be more physically based and still require a reasonable amount of data (Martinec and de Quervain 1975).

In whatever manner snowmelt models are adapted or developed for use over large, cold region basins, areally distributed data will be required. Because of difficulty in acquiring such information conventionally, the use of remote sensing is mandatory for such large-area applications. Appropriate remotely sensed data are already being collected, and additional data sources are under development. Snowcover extent, as obtained operationally from NOAA-AVHRR and GOES satellites, is mapped for over 4000 river basins in North America by the National Operational Hydrologic Remote Sensing Center (NOHRSC) of the US National Weather Service. Additionally, NOHRSC produces snow water equivalent maps based largely on airborne gamma ray snow surveys (Carroll, 1995).

Satellite microwave data over snow are also being acquired. SSM/I data are being gridded, archived and distributed by the World Data Center-A for Glaciology in Boulder, Colorado. Much research remains to be done to produce operational products, but initial results show much promise for obtaining all-weather snowcover extent and, eventually, snow water equivalent. One problem inherent in the SSM/I data is poor resolution (e.g. 25 km at 37 GHz). Empirical snow water equivalent algorithms for use with SSM/I data exist, but accounting for the strong effects of variations in grain size and shape on the determination of snow water equivalent has not yet been solved. An improvement in resolution (8 km at 37 GHz) may be possible by 1996 when data from the Russian PRIRODA experiment become available. Eventually, areal data on snowcover extent, snow water equivalent, the onset of snow melting and perhaps frozen soil extent should be available from passive microwave satellite data.

Refinements and additions to data available from visible and infrared satellite sensors are already being pursued. Areal information on cloud cover and radiative fluxes may be added to the operational areal snow extent information (Simpson, 1995; Simpson and Gobat, 1995).

Some hydrological models are capable of generating snow-covered area information in their snow accumulation and ablation calculations. Such snow extent information is now reliably available from several remote sensing sources (Carroll, 1990; Baumgartner and Rango, 1991). At a minimum, all operational snowmelt runoff models need to incorporate remotely sensed snowcover extent information. Operational forecasting models may accept snowcover extent as a direct input. In process-based models whose primary goal is physical understanding rather than operational forecasts, variables such as snow-covered area constitute model response, rather than model inputs; in such cases, remotely sensed snow observations should be used to test and diagnose the models' performance. Kirnbauer *et al.* (1994) find that snowcover depletion patterns are 'vastly superior to runoff data' for testing model assumptions and parameters.

This paper describes the first step in combining temperature and radiation data in a widely used degree–day model, the snowmelt runoff model (SRM), which incorporates remotely sensed snowcover extent data. In this study, measured radiation data from a very small research basin are used to demonstrate that the combined temperature and radiation index approach can successfully simulate the runoff hydrograph, while reducing the number of parameters that must be estimated. The ultimate goal is to extend this approach to large basins using modelled radiation (Kustas *et al.*, 1994) and actual remotely sensed measurements of necessary model inputs.

SNOWMELT RUNOFF MODEL SIMULATIONS INCORPORATING RADIATION MEASUREMENTS

Snowmelt runoff model

The snowmelt runoff model (SRM) is used worldwide for forecasting melt season runoff in mountain regions. SRM has been developed for microcomputer application (Martinec *et al.*, 1994). It is ideal for use in data-sparse regions (Kumar *et al.*, 1991) owing to its simple data requirements and use of remote sensing to determine snow-covered area. SRM has been used successfully to simulate runoff in over 60 basins ranging from 0·76 to 122 000 km^2 in area. The model has also been used to evaluate the effects of climate change on regional water supply (Rango, 1992).

The SRM uses a temperature index (degree–day) approach to melt snow from a basin's elevation zones. As a single meteorological variable for predicting snowmelt, air temperature has been shown to be the best index (Zuzel and Cox, 1975). The degree–day approach has been criticized as lacking a physical basis in comparison to more complete energy balance approaches. None the less, degree–day methods remain popular in snowmelt modelling, and perform well when properly applied (Rango and Martinec, 1995).

SRM requires a measurement or prediction of snow-covered area as an input to the melt calculations. For simulations, the required snowcover data are obtained from the remote sensing images. In climate change or forecast modes, the SRM automatically evaluates the future course of snowcover depletion by deriving curves of snow-covered area versus cumulative melt (modified depletion curves) from records of snow-covered area versus time (conventional depletion curves). This procedure is described in Martinec *et al.* (1994).

Combining the surface radiation budget with the temperature index shows promise for developing an operational, yet more physically based snowmelt model (Martinec and de Quervain, 1975). A new version of the SRM incorporating net surface radiation is under development; depending on data availability, the user could choose between the simple temperature index or the slightly more complex temperature and radiation versions.

Presumably, a radiation index model should perform best where net radiation is measured, rather than estimated from meteorological variables. In this study, a new research version of the SRM incorporating net radiation is tested on a small basin where simultaneous measurements of air temperature, surface radiation and streamflow are available.

Degree–day and restricted degree–day versions of SRM

A schematic diagram (Figure 1) shows SRM's input requirements, parameters and computational algorithm. The components appearing below the large dashed line represent the current version of the SRM (version 3.2) (Martinec *et al.*, 1994). Above the dashed line are the new radiation-based components.

The basin is subdivided into hydrological response units (HRUs). In the current version (3.2) of the

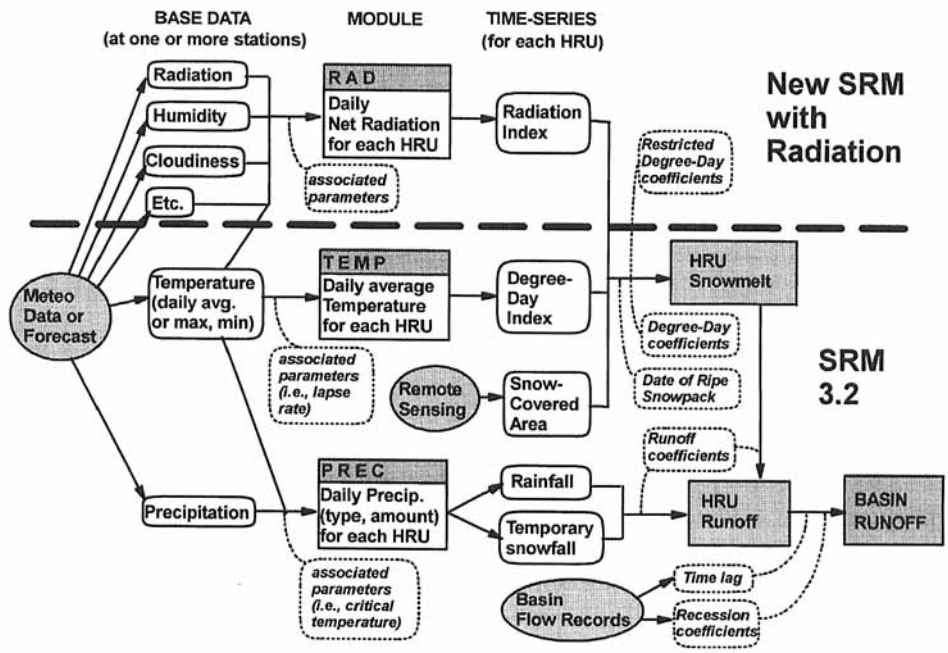

Figure 1. A schematic diagram of the snowmelt runoff model (SRM) computational algorithm. The current version of SRM appears below the large dashed line; above the dashed line are the additional input data and computational module for the new radiation-based version

SRM, the HRUs consist of elevation zones; with the addition of the radiation component, aspect (orientation) must be considered as well as elevation in subdividing the basin into HRUs.

The computational modules TEMP and PREC extrapolate measured or forecast data to each of the HRUs. SRM 3.2 then computes the snowmelt contribution from the snow-covered fraction of each HRU as proportional to the HRU temperature (degree–day) index,

$$M = aT_d \tag{1}$$

where T_d (°C) is the degree–day index and a (cm day^{-1} °C^{-1}) the degree–day coefficient. The SRM then combines the melt contributions with direct rainfall runoff from each HRU, and routes the respective contributions to the basin outlet.

In the new version of the SRM, the added computational module RAD calculates net surface radiation for each elevation/aspect HRU from measured and/or model-calculated components of the radiation budget. The available data dictate the selection between several possible computational routines; these data and routines are shown schematically in Figure 1. The SRM snowmelt calculation then multiplies the degree–days by a restricted degree–day coefficient (a_r) and adds a melt contribution proportional to a net radiation index, R_d [W m^{-2}],

$$M = m_Q R_d + a_r T_d \tag{2}$$

In Equation (2), m_Q [(cm day^{-1}) (W m^{-2})$^{-1}$] is a physical constant converting energy to water mass or depth, and a_r (cm day^{-1} °C^{-1}) is the restricted degree–day coefficient, which is not equal to a in Equation (1) but multiplies the same T_d. The HRU snowmelt amounts are combined with rainfall runoff and routed to the basin outlet as before.

In the degree–day version of SRM (version 3.2, hereafter called DD), the degree–day coefficient a varies (generally increasing) throughout the melt season. This time varying parameter is evaluated from physical properties of the snowpack and the basin, and is not used to calibrate the model. Observations have shown that the restricted degree–day coefficient a_r in Equation (2) is less variable in time than a in Equation (1) (Martinec, 1989). In addition, a_r may be estimated from representative meteorological data where lysimeter melt measurements are not available (see Appendix).

Study site and data

The streamflow, temperature and radiation data used in this study are from the W-3 sub-basin of the Sleepers River Research Watershed near Danville, Vermont, for the years 1969–1974 (Anderson *et al.*, 1977). The data set includes measurements from the former NOAA-ARS Snow Research Station, now operated by the US Army Corps of Engineers Cold Regions Research and Engineering Laboratory (Hardy, 1994). The W-3 basin is 8·42 km^2 in area, with an elevation range from 346 to 694 m a.s.l.; its hypsometric mean elevation is 498 m a.s.l. The Snow Research Station lies at 552 m a.s.l. Because of its small area and elevation range, the W-3 basin is not subdivided by elevation or aspect in this study; i.e., it is treated as a single HRU.

Methods and assumptions

The TEMP and PREC modules used in this study are the current standards for the SRM (Martinec *et al.*, 1994). Because daily radiation measurements are available for the Sleepers River Research Watershed, the RAD module used here is a simple sum of components; alternative RAD modules in future versions of SRM will incorporate the model described by Kustas *et al.* (1994) and other developments.

Temperature module (TEMP). Daily average, base station temperature T_a is taken as $0{\cdot}5(T_{max} + T_{min})$ and lapsed to the hypsometric mean elevation of the HRU using a lapse rate of 0·65°C/100 m. The degree–day index T_d is equal to the HRU daily average temperature, or 0°C, whichever is greater,

$$T_d = \max[T_a, 0] \tag{3}$$

Precipitation module (PREC). SRM 3.2 assumes that the measured base station precipitation volume is uniform over the basin, and the type (snow or rain) uniform over each elevation zone or HRU. If the HRU

daily average temperature is below a critical value (here, 0·75°C), the day's precipitation is assumed to be in the form of snow.

Radiation module (RAD). For this study, daily net radiation at the base station is calculated as follows,

$$R_{net} = K_{in} - K_{ref} + L_{in} - L_s \tag{4}$$

where R_{net} is net radiation flux density (W m^{-2}), K_{in} is incident short-wave (solar) radiation, both direct and diffuse, K_{ref} is short-wave radiation reflected by the snow surface (albedo × K_{in}), L_{in} is incident long-wave radiation emitted by the overlying atmosphere and L_{surf} is long-wave radiation emitted by the snow surface.

Daily incident short-wave and daily average albedo are taken from the Snow Research Station observations reported by Anderson *et al.* (1977), with the exception that in this study the albedo is not allowed to fall below a certain minimum value, by the following reasoning and procedure. As the snow disappears from the ground beneath the radiometer, the albedo measurements become quite small, owing to partial snow coverage. The melt calculation of the SRM is made only for the snow-covered area, thus, when the reported albedo falls below 0·35, it has been assigned the value 0·35 in this study.

Incoming (atmospheric) long-wave radiation, L_{in}, is the most difficult input variable to measure. Anderson (1976) describes the problems with the pyrgeometer used at Sleepers River during the study years; in particular, the instrument records too high when its dome oxidizes, and when skies are clear. This study follows Anderson (1976) and uses estimated values of L_{in}, rather than the direct measurements. The values of L_{in} reported by Anderson (1976) were computed from air temperature, vapour pressure and the ratio of incoming solar radiation to clear sky radiation by the method suggested by Anderson and Baker (1968). These values of L_{in} are consistent over the study period, and compared well with the pyrgeometer measurements when the instrument was new and short-wave radiation was low (Anderson, 1976).

The surface-emitted long-wave radiation, L_{surf}, is calculated by the Stefan–Boltzmann law, using an emissivity of 0·99. Daily average snow surface temperature measurements are available for about half of the days of the study's snowmelt seasons, more in some years than others. Snow surface temperature was measured hourly, with a thermocouple at the snow surface in 1969, and with an infrared thermometer in the remaining years. The daily average snow surface temperature, T_s, is reported (Anderson, 1976) only for days with full hourly records. In this study, for the days on which T_s is missing, a relationship between daily average air temperature (T_a) and daily average snow surface temperature (T_s) is assumed, derived from the available data:

$$T_s = \min[T_a - 2{\cdot}5, 0] \qquad [°C] \tag{5}$$

Equation (5) is based on inspection of a plot of daily average snow surface temperature against daily average air temperature (Figure 2), for those days in the record when (a) snow surface temperature was measured with an infrared thermometer, and (b) both air and snow surface temperature were recorded at every hour of the day.

In this study, net radiation is assumed uniform over the basin. No topographic or vegetation related adjustments are applied to any components of R_{net}. In other words, module RAD consists here of a simple sum of input time-series of K_{in}, K_{ref}, L_{in} and L_{surf}, as measured or computed at the Snow Research Station (552 m a.s.l.). Because the basin relief is only 350 m, the air temperature is assumed to vary from its value at the station by no more than about 1·5°C (applying a lapse rate of 0·65°C/100 m), which introduces a maximum error of 2% in the long-wave radiation T^4 terms. Implicit parameters are those used in the assumed T_s [Equation (5)] and those of the Anderson–Baker (1968) model. The radiation index R_d in the RDD model [Equation (2)] is set equal to R_{net} if greater than zero, and to zero otherwise,

$$R_d = \max[R_{net}, 0] \quad [W m^{-2}] \tag{6}$$

Snowmelt and snow-covered area. The restricted degree–day version of SRM calculates daily snowmelt by Equation (2). This melt depth is assumed uniform over the snow-covered fraction of the HRU. Areal snowcover, generally obtained from satellite images, is a critical input to the SRM. Because W-3 is too small for use of the more common satellite data available during this time period, snow-covered area was estimated from transect snow surveys as reported by Anderson *et al.* (1977) at several elevations in the basin. As discussed in the SRM user's manual (Martinec *et al.*, 1994), the snowcover depletion curves were

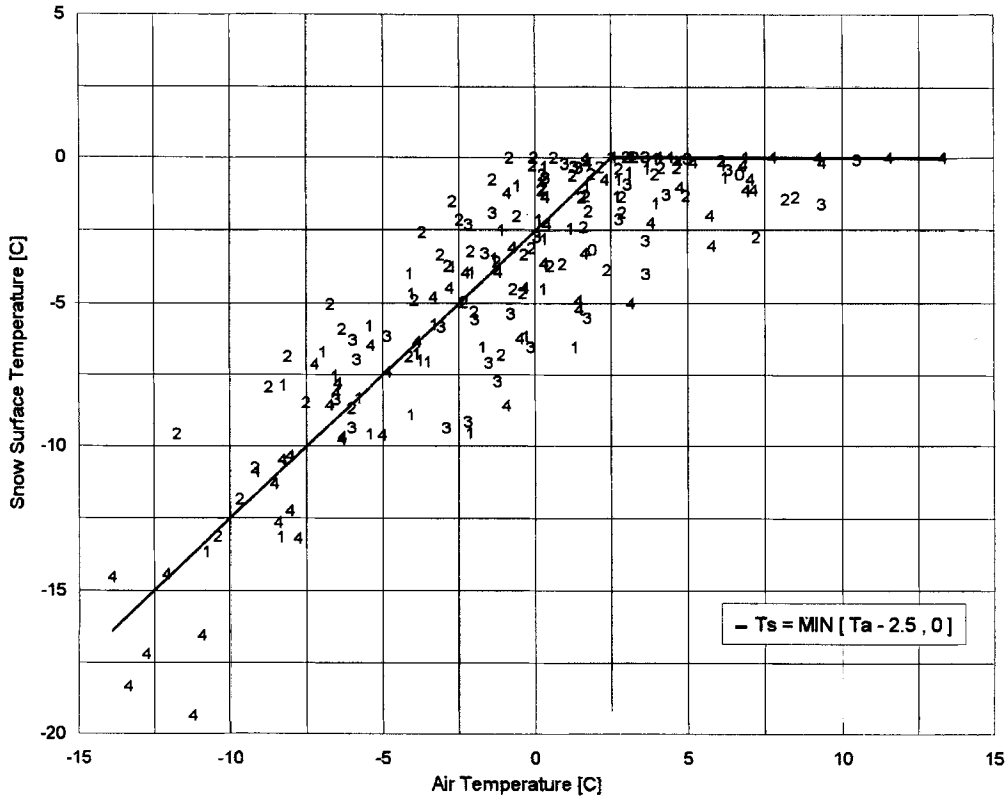

Figure 2. Scatter plot of daily average air temperature versus daily average snow surface temperature at the Sleepers River Snow Research Station (Vermont) for the years 1970–1974. The symbols '0' to '4' indicate the year. Snow surface temperature was measured by infrared thermometer. Averages were computed from hourly observations, and are shown only for days on which the complete hourly record was available for both temperatures. The solid line indicates the relationship assumed for days on which measured average snow surface temperature was not available. Data from Anderson *et al.* (1977)

adjusted as necessary to account for new, short-lived snowfall that occurred after seasonal snowmelt began.

Runoff. The algorithm that transforms melt and rainfall into basin outflow is identical to that used in the current version of SRM (Martinec *et al.*, 1994).

Model parameters and input data. Simulation runs using both the DD and RDD version of SRM are

Table I. SRM degree-day coefficients for W-3 basin

Time period		Degree-day coefficient* a						Restricted degree-day coefficient† a_r
		1969	1970	1971	1972	1973	1974	(all 6 years)
March	1–15	0·3	0·35	0·3	0·3	0·4	0·4	0·2
	16–31	0·35	0.35	0·35	0.35	0·4	0·45	0·2
April	1–15	0·4	0·4	0·4	0·4	0·45	0·45	0.2
	16–30	0.45	0.45	0·45	0·45	0.55	0·5	0·2
May	1–15	0·55	0·55	0.5	0.5	0.55	0.55	0·2

* From snow density data

† From meteorological data, as described in the Appendix

compared for six snowmelt seasons in the W-3 basin. In each pair of simulations, all inputs and parameters are the same, except that for RDD the radiation index is included and the time-varying a is replaced with a constant a_r (Table I); this value was determined as described in the Appendix. The runoff parameters were estimated and assigned based on physical considerations and basin records. Naturally, simulation results could be improved by tuning a_r (or any model parameters), but that would be counter to the modelling philosophy that 'the SRM parameters are not calibrated or optimized by historical data. They can be either derived from measurement or estimated by hydrological judgment taking into account the basin characteristics, physical laws and theoretical relations or empirical regression relations... .' (Martinec *et al.*, 1994).

Simulation results

Runoff hydrographs comparing measured flow to that computed by both model versions are presented in Figure 3. The flow computed by the two model versions becomes identical after the snowcover disappears.

In addition to the hydrographs, the simulation accuracy is evaluated for each year (Table II) using two measures: the coefficient of determination R^2 and the volume difference D_v. R^2 is computed as follows:

$$R^2 = 1 - \frac{\Sigma_{i=1}^{n}(Q_i - Q_i')}{\Sigma_{i=1}^{n}(Q_i - \bar{Q})} \tag{7}$$

where Q_i are Q_i' are the measured and computed daily discharge, respectively, $\bar{Q}$ the average measured discharge for the given year or melt season and n the number of daily discharge values. The volume difference D_v is defined as

$$D_v[\%] = \frac{V_R - V_R'}{V_R} \times 100 \tag{8}$$

where V_R is the measured and V_R' the computed yearly or seasonal runoff volume. A non-zero D_v may result from errors in model input (i.e. extrapolation of temperature measurements, snow-covered area), errors in the runoff parameters (i.e. evaporative loss) or physical factors (gauge catch deficit or point precipitation measurements that are not representative of precipitation over the basin).

The comparison for 1969 (Figure 3a) shows the most improvement, according to both computed performance measures (Table II), mostly by better capturing the flow in late March to early April, predicting a higher peak at 10 April, and higher flow rates from 20 April to the disappearance of snowcover in mid-May. Both models miss the runoff spike at 19 April, possibly owing to spatial variability or gauge catch deficit in the precipitation event of 18–19 April.

The major difference between the model versions for 1970 (Figure 3b) is the overestimation by RDD of the flow between 9 and 16 April. At first examination, this difference appears to be a more correct prediction of snowmelt by DD for this period. However, the rising limbs of the two model hydrographs start from different flow rates on 7 April, and this appears to explain much of the difference. If the SRM is initialized with the measured flow on 7 April, then DD also overpredicts runoff for this period. This error apparently

Table II. SRM performance measures: W-3 basin

Year	R^2		Simulation over (−) or under (+) estimation of seasonal flow D_v (%)	
	DD	RDD	DD	RDD
1969	0·79	0·86	20	10
1970	0·84	0·79	19	−1·9
1971	0·91	0·93	5·8	0·66
1972	0·85	0·82	17	0·21
1973	0·63	0·52	12	3·4
1974	0·75	0·74	15	1·9

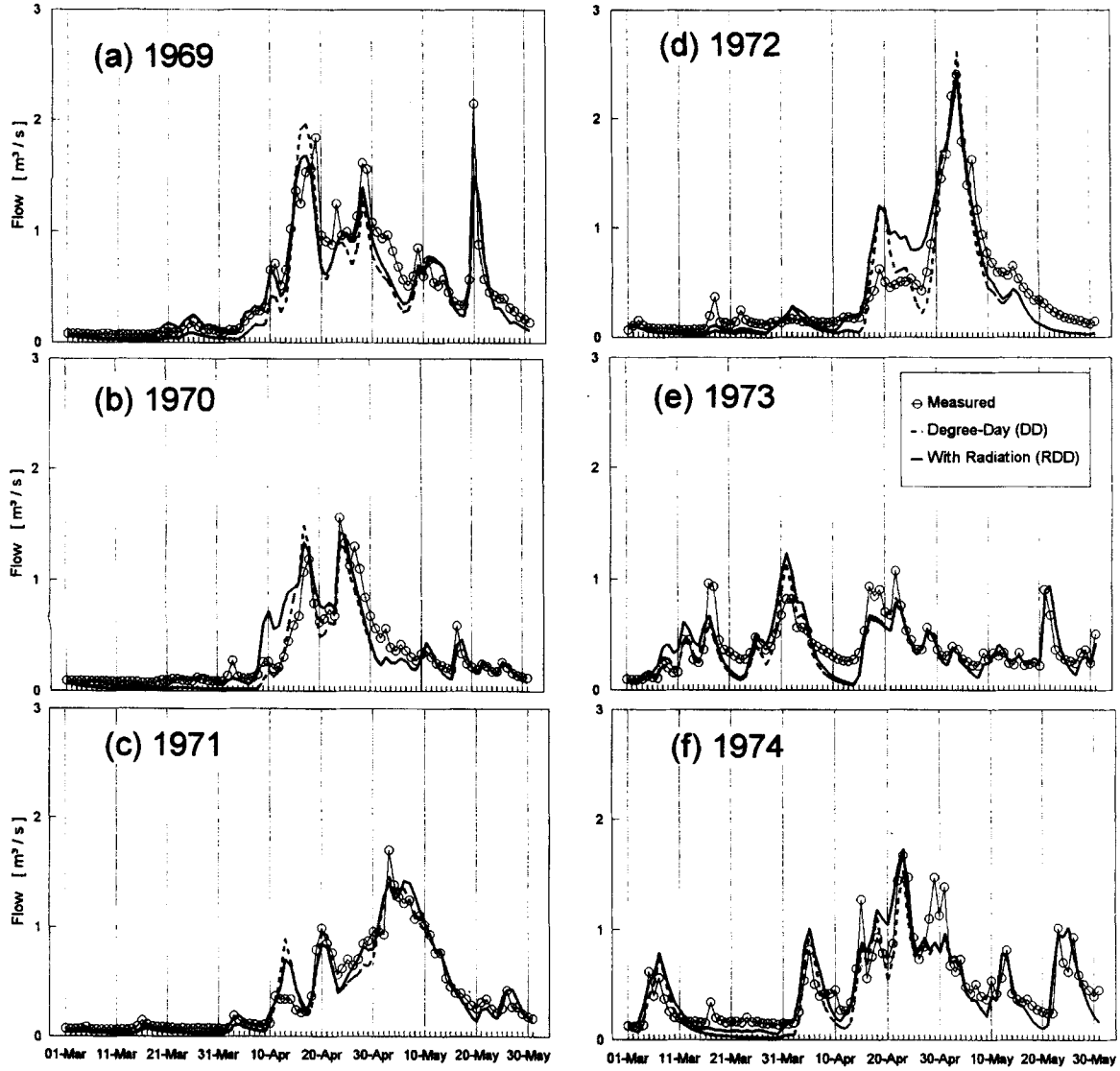

Figure 3. Hydrographs for the W-3 basin, 1969–1974. Observed (open circles) and simulated using the SRM (dashed line: degree–day only; solid line: restricted degree–day, including net radiation)

has to do with how SRM stores and melts the snow event of 2–3 April, as well as the recession parameterization of the SRM; these treatments are identical in DD and RDD. This initialization sensitivity is discussed in the following section.

In 1971 (Figure 3c), a slight improvement in R^2 and D_V comes about, as in 1969, through higher flow rates before 10 April and from 23–30 April. Both models overpredict the runoff peak at 13 April. Snow surface temperature is estimated by Equation (5) for 11, 12 and 14 April; more accurate information on T_s might allow RDD to make more improvement over DD for this period. In addition, the energy required to warm the snowpack from a daily average surface temperature of −8°C on 8 April to 0°C on 10 April is erroneously assigned to snowmelt by both models.

Both models overestimate the runoff between 18 and 21 April 1972 (Figure 3d), but the overestimation persists in RDD. Possibly, RDD is overpredicting runoff throughout this period by producing melt from positive net radiation, although the snow surface temperature remains below freezing throughout the

day for several days of the period. Because the daily average air temperature is below freezing on these days, neither DD nor RDD produces melt from the T_d term.

In 1973 (Figure 3e), the snow cover was depleted several weeks earlier than in the other study years. The hydrograph reflects a warm, rainy spring with little seasonal snowmelt signature, and both versions of the SRM perform poorly.

In 1974 (Figure 3f) RDD makes a slight improvement in R^2 and reduces the volume error. Again, the missed runoff peaks at 15 April, 29 April and 1 May might be attributed to gauge catch deficit or spatial variability in precipitation over the basin.

In two of the six years, the RDD model improves the goodness-of-fit measure R^2 by up to 0·07 (1969); in the other three years, R^2 decreases, by 0·11 in 1973, which is also the worst performance of the DD model, by this measure. In all six years, the volume difference (D_V) is significantly decreased in the RDD runs, with respect to the DD runs, which consistently underestimated seasonal flow. This result suggests that using the same restricted degree–day coefficient throughout the melt season of any year produced nearly an unbiased estimate of the volume of runoff on a seasonal basis and that the value of a_r derived from physical arguments (see Appendix) is reasonable.

Forecasts with periodic updating

Model sensitivity to initial flow values was discussed above in connection with Figure 3b. The SRM partitions daily meltwater production and rainfall into immediate runoff and baseflow according to a recession parameterization, whereby the streamflow for day i, Q_i, is computed as (schematically),

$$Q_i = \begin{pmatrix} \text{daily melt and} \\ \text{rainfall contribution} \\ \text{from all zones} \end{pmatrix} (1 - k_i) + Q_{i-1} k_i \tag{9}$$

where k_i is the recession coefficient for day i. (For further details, see Martinec *et al.*, 1994.) Thus, an error in a daily streamflow value continues to propagate to the following days' predicted flow. As a result, the seasonal simulations do not isolate the differences or similarities between the DD and RDD methods of computing daily melt. SRM allows the option of running in periodic updating mode, i.e. the streamflow Q_{i-1} is set to its measured value every n days, where n may be a value from 1 to 9. Setting n equal to 1 creates a one-day forecast, i.e. the SRM calculates the streamflow for day i based on that day's temperature and net radiation indices, given a known streamflow for day $i - 1$. When both versions of the model are run in this mode, all differences between the results are due to the daily melt formulation alone, not the accumulation of initialization error. Figure 4 shows the one-day forecasts for 1970. RDD (with a constant a_r)

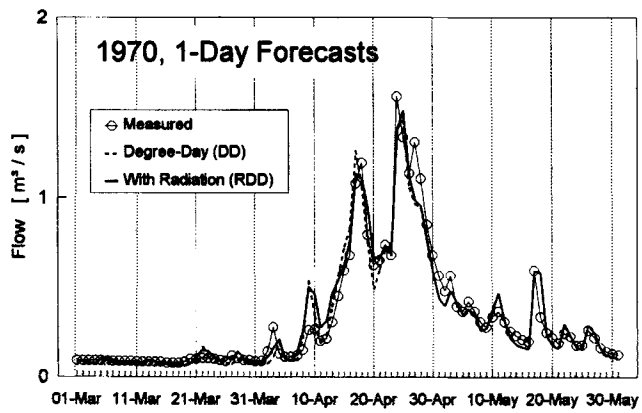

Figure 4. One-day forecast hydrographs for the W-3 basin in 1970. Observed (open circles) and simulated using the SRM, with streamflow updated daily (dashed line: degree–day only; solid line: restricted degree–day, including net radiation)

Table III. Model accuracy with periodic updating

	R^2											
	1969		1970		1971		1972		1973		1974	
	RDD	DD	RDD	DD	RDD	DD	RDD	DD	RDD	DD	RDD	DD
No update	0·86	0·79	0·79	0·84	0·93	0·91	0·82	0·85	0·52	0·63	0·74	0·75
Nine-day	0·84	0·78	0·81	0·86	0·92	0·9	0·85	0·84	0·61	0·66	0·72	0·72
Five-day	0·88	0·83	0·88	0·88	0·93	0·9	0·89	0·88	0·65	0·69	0·77	0·75
One-day	0·89	0·87	0·94	0·94	0·94	0·94	0·96	0·94	0·8	0·82	0·79	0·8

and DD (with a time varying a) produce very similar daily melt rates and one-day flow forecasts throughout the 1970 season, supporting the claim that the differences apparent in Figure 3 are due to flow initialization error, not differences in the melt algorithm.

Table III presents the R^2 values for the six study years, with periodic updating at 1, 5 and 9 days. In three of the years when the simulation (no update) R^2 decreased in going from DD to RDD (1970, 1972 and 1973), the differences between the DD and RDD R^2 are reduced or eliminated in the one-day forecast. In 1974, the R^2 differ by 0·01 in both the full simulation and the one-day forecast. It is interesting to note that in three of the study years (1969, 1971 and 1972), the nine-day update does *not* improve either model's accuracy with respect to the full (no update) simulation, indicating that some compensating error must be occurring in the full simulation. The five-day update improves the model accuracy in all years except 1971.

Discussion

In the full simulation mode, the new version of the SRM incorporating measured radiation data for the W-3 research basin improves R^2, with respect to the temperature index version, in two of six study years. In the remaining study years, R^2 is decreased by 0·01 (1974) to 0·11 (1973). Improvements in the runoff volume difference, D_V, are noted in all six study years. In one-day forecast mode, the two model versions perform similarly. Advantages of the radiation-based method are (1) improved physical representativeness of the algorithm, separating radiation and turbulent energy inputs to the snowpack; (2) less variability in the coefficient multiplying the temperature (degree–day) index; and (3) the potential for a physically based methodology (see Appendix) to estimate the restricted degree–day coefficients from representative meteorological values when snow density or lysimeter melt measurements are not available.

Anderson (1976) recommends that snowmelt index models should keep the number of indices to a minimum, because of interrelationships between the indices. In a degree–day model, the single temperature index must account for all the physical processes in the energy budget, including both turbulent and radiative energy exchange. The two-index version of SRM proposed here accounts for the different forms of energy exchange through Equation (2). The degree–day or temperature index is thus only required to account for the turbulent flux contribution to melt. The radiation and temperature indices are correlated, owing to the physical cause and effect relationships between net radiation and surface and air temperature. This correlation would be a drawback in a purely statistical or regression model using the two indices, because such a model could not distinguish between the physical contributions of the two terms. However, Equation (2) separates the indices into separate contributions to melt, and allows determination of parameters based on physical considerations. Therefore, redundancy or overlap between the two indices is reduced.

The use of a threshold for each respective index [Equations (3) and (6)] may result in situations where the index equation [Equation (2)] overestimates the energy available for snowmelt. For example, consider a situation with net radiation into, and net turbulent fluxes away from the snowpack. In that case, R_d would be positive ($R_{net} > 0$) while T_d would be 0 ($T_a < 0$). If the full energy budget were considered, the turbulent flux energy loss would essentially cancel part of the radiative input, reducing the energy available for melt, but Equation (2) would indicate melt proportional to R_{net}. The reverse situation is possible as well:

net radiation out of, and turbulent fluxes into the snowpack, forcing R_d to equal 0, but producing melt proportional to T_d, again overestimating the energy available for melt. However, both cases are probably likely to occur only early in the melt season, when both R_d and T_d are small.

During the melt season, the latent and sensible turbulent fluxes may be in opposite directions, as when the air is warm and dry. In such cases, the net turbulent energy flux is small, and the melt process is dominated by net radiation. If such conditions were typical of the basin, the seasonally representative a_r (computed as suggested in the Appendix) would account for this effect. In applications of the RDD model, therefore, it is critical that a_r reflect the climatic conditions of the basin.

Computing the net radiation term requires a measurement or estimate of snow surface temperature. The snow surface temperature must necessarily be 0°C when the snow is actively melting, generally during only part of the day. However, because the air and snow cool at night, the daily average T_s can easily fall well below 0°C, even well into the melt season (Baker *et al.*, 1996). The net radiation term reflects a 24 hour average; therefore, the daily average snow surface temperature should be used in estimating L_{surf} for RDD. As an example of the sensitivity of R_{net} to T_s, assuming a snow surface temperature of 0°C rather than −10°C in the upwelling long-wave flux would result in overestimating L_{surf} by 40 W m^{-2}, which is sufficient to change the sign of net radiation early in the melt season. Unfortunately, given $T_s < 0$°C, a single daily average T_s cannot distinguish between a day when the snow surface attains $T = 0$°C for part of the day and melt occurs, and a day when it does not (as in the 1972 simulation). A possible improvement would involve estimating $T_{s\,max}$ and $T_{s\,min}$ for the snow surface (based on near-surface air temperature measurements or remote sensing of the surface), then disallowing any melt from either the T_d or the R_d contribution on days when $T_{s\,max}$ is below 0°C. The non-representativeness of point measurements or estimates of snow surface temperature is a problem.

Finally, because the air temperature rarely follows a perfectly sinusoidal course throughout the day, approximating T_a as 0·5 ($T_{max} + T_{min}$) may tend to misrepresent or bias daily average temperature, and thus daily melt as well, through both the temperature and the radiation index. However, SRM users rarely have access to full hourly temperature records that would allow more accurate estimates, and such errors must be accepted when using SRM and similar operational models.

SUMMARY

Initial testing of the new radiation-based version of SRM using measured radiation for the W-3 basin of Vermont shows promising results. In full simulation of runoff from the W-3 basin, the net radiation/degree–day combined version of SRM produced improvements in R^2, with respect to the degree-day approach alone, in two of six snowmelt seasons; in the remaining years, R^2 declined by up to 0·11 in going from the degree–day to the radiation version. Improvements in percentage volume error were noted in all six study years. The RDD and DD approaches performed similarly in one-day forecasts, which eliminate the accumulation of initialization error. The possibility of replacing the time varying degree–day coefficient with a constant restricted degree–day coefficient represents an improvement from an operational point of view.

It is unlikely that measurements of all the short- and long-wave components of net radiation would be available for SRM application to an arbitrary basin. Additionally, for large basins, point radiation measurements or estimates could not be assumed to represent the whole basin, as in this study. None the less, the results using measured radiation for the W-3 basin suggest that a good radiation model could produce similar improvement where radiation measurements are not available.

A radiation module is being incorporated into SRM; this module will allow the user to choose between several approaches, depending upon available data. At a minimum, air temperature (which SRM already requires) and some estimate of cloud cover are required to estimate net radiation; measurements of humidity and any components of the radiation budget, such as global short wave, would improve the estimate. An alpine snow cover analysis system is under development, integrating remote sensing data, image processing and geographic information systems (Baumgartner and Rango, 1995). This system will improve snow mapping input to SRM by hydrological response units defined on the basis of elevation and general aspect, and

incorporate relevant remotely sensed information (such as albedo, surface temperature and cloud type and amount), as these data continue to become operationally available.

The new approach shows promise for employing net radiation effectively and efficiently in snowmelt runoff estimation. With the addition of a net radiation index to the SRM, the already small number of parameters that must be estimated is reduced further. The new SRM should be better suited for climate change evaluations if general circulation models can provide reliable climate change scenarios that include changes in temperature, precipitation, cloud cover, humidity and radiation.

ACKNOWLEDGEMENTS

This research is supported in part by the Electric Power Research Institute, Palo Alto, California. We thank D. Tarboton and J. Copeland for their helpful comments on an earlier version of the manuscript.

REFERENCES

Anderson, E. A. 1976. 'A point energy and mass balance model of a snow cover', *NOAA Technical Report NWS 19*. US Department of Commerce, Washington, DC.

Anderson, E. A. and Baker, D. R. 1968. 'Estimating incident terrestrial radiation under all atmospheric conditions', *Wat. Resour. Res.*, **3**, 975–988.

Anderson, E. A., Greenan, H. J., Whipkey, R. Z., and Machell, C. T. 1977. 'NOAA-ARS cooperative snow research project: watershed hydro-climatology and data for water years 1960–1974', *NOAA–S/T 77-2854*. US Department of Commerce, Washington, DC.

Baker, J. M., Flerchinger, G. N., and Spaans, E. J. A. 1996. 'Sensible heat exchange during snowmelt: measurement and simulation', Preprint volume of American Meteorological Society, *22nd Conference on Agricultural and Forest Meteorology with Symposium on Fire and Forest Meteorology and 12th Conference on Biometeorology and Aerobiology, Atlanta, GA*, pp. J8–J11.

Baumgartner, M. F. and Rango, A. 1991. 'Snow cover mapping using microcomputer image systems', *Nord. Hydrol.*, **22**(4), 193–210.

Baumgartner, M. F. and Rango, A. 1995. 'A microcomputer-based alpine snow cover analysis system', *Photogramm. Engng Remote Sensing*, **61**, 1475–1486.

Carroll, T. R. 1990. 'Remote sensing of snow in cold regions', *Proceedings, First Moderate Resolution Imaging Spectroradiometer (MODIS) Snow and Ice Workshop*. NASA Conference Publication CP-3318, NASA/Goddard Space Flight Center, Greenbelt, Maryland, USA. pp. 3–14.

Carroll, T. 1995. 'Mapping snow water equivalent and snow cover in North America', *International GEWEX Workshop on Cold Season/Regions Hydrometeorology, Banff, Alberta, Canada.*

Hardy, J. 1994. 'Solar and terrestrial radiation data from the Sleepers River Research Watershed, a summary report', *Special Report 92–94*, US Army Corps of Engineers Cole Regions Research and Engineering Laboratory, Hanover, NH.

Kirnbauer, R., Blöschl, B., and Gutknecht, D. 1994. 'Entering the era of distributed snow models', *Nord. Hydrol.*, **25**, 1–24.

Kumar, V. S., Haefner, H., and Seidel, K. 1991. 'Satellite snow cover mapping and snowmelt runoff modeling in Beas Basin', in *Snow, Hydrology and Forests in High Alpine Areas (Proceedings of the Vienna Symposium), IAHS Publ.*, **205**, 101–109.

Kustas, W. P., Rango, A, and Uijlenhoet, R. 1994. 'A simple energy budget algorithm for the snowmelt runoff model', *Wat. Resour. Res.*, **30**, 1515–1527.

Martinec, J. 1989. 'Hour-to-hour snowmelt rates and lysimeter outflow during an entire ablation period', *Snow Cover and Glacier Variations (Proceedings of the Baltimore Symposium, Maryland, May 1989). IAHS Publ.* **183**, 19–28.

Martinec, J. and de Quervain, M. R. 1975. 'The effect of snow displacement by avalanches on snow melt and runoff', in *Snow and Ice Symposium (Proceedings of the Moscow Symposium, August 1971; Actes du Colloque de Moscou, August 1971). IAHS-AISH Publ.* **104**, 364–377.

Martinec, J., Rango, A., and Roberts, R. 1994. *Snowmelt Runoff Model (SRM) User's Manual*. Geographica Bernensia, P29, Department of Geography, University of Bern. 65 pp.

Morris, E. M. 1989. 'Turbulent transfer over snow and ice', *J. Hydrol.*, **105**, 205–223.

Rango, A. 1992. 'Worldwide testing of the Snowmelt Runoff Model with applications for predicting the effects of climate change', *Nord. Hydrol.*, **23**, 155–172.

Rango, A. and Martinec, J. 1995. 'Revisiting the degree day method for snowmelt computations', *Wat. Resour. Bull.*, **31**, 657–669.

Simpson, J. L. 1995. 'Improved satellite estimates of cloud cover, radiative fluxes, and areal extent of snow cover for use in hydrometeorologic studies', *International GEWEX Workshop on Cold Season/Regions Hydrometeorology, Banff, Alberta, Canada.*

Simpson, J. J. and Gobat, J. I. 1995. 'Improved cloud detection in GOES scenes over land', *Remote Sensing Environ.*, **52**, 36–54.

Zuzel, J. F. and Cox, L. M. 1975. 'Relative importance of meteorological variables in snowmelt', *Wat. Resour. Res.*, **11**, 174–176.

APPENDIX

Physical basis and estimation of the restricted degree–day factor

Empirical methodology exists to compute or estimate the degree–day parameter, a, for the current version of SRM from snow density data, where lysimeter measurements are not available (Martinec *et al.*, 1994).

Such methodology has not yet been developed for the restricted degree–day parameter, a_r, required by the new radiation-based version. This appendix describes a method to estimate a_r from representative meteorological characteristics of the basin, based on an approximation to the full snowmelt energy budget equation.

Assuming negligible change in the energy storage of the snowpack, and negligible energy transfer between the snow and the ground during the melting phase, the energy budget of the snowpack is expressed by

$$\Delta Q = R_{net} + H + LE \tag{A1}$$

where ΔQ is the energy used to melt snow, R_{net} is net radiation and H and LE are, respectively, the turbulent fluxes of sensible and latent heat into the snowpack. Using the standard bulk transfer parameterization, the turbulent fluxes are functions of the surface layer gradients in temperature and humidity, wind speed and boundary layer stability:

$$H = \rho C_p C_h k^2 (\ln z/z_0)^{-2} u(T_a - T_s) \tag{A2a}$$

$$LE = \rho L C_e k^2 (\ln z/z_0)^{-2} u(q_a - q_s) \tag{A2b}$$

in which ρ is the density of air, C_p the specific heat of air at constant pressure, k is the von Karman constant, z and z_0 are the measurement and roughness heights, respectively, u is the wind speed, L is the latent heat of vaporization, T and q are the temperature and specific humidity, with subscript a indicating measurement height and s the snow surface, and C_h and C_e are the stability corrections to the bulk transfer coefficient for sensible and latent heat, respectively. The details of the bulk transfer approach used here are given in Kustas *et al.* (1994). It is assumed that

$$C_e = 0{\cdot}5 C_h \tag{A3}$$

following the findings of Morris (1989) for turbulent transfer over ice and snow. The specific humidity at measurement height may be expressed in terms of the relative humidity and the saturation vapour pressure,

$$q = RHq^* = RH \frac{0{\cdot}622}{p} e^* \tag{A4}$$

where RH is the relative humidity, q^* the saturation specific humidity, p the surface air pressure and e^* the saturation vapour pressure. The saturation vapour pressure (a function of temperature) may be approximated in a truncated Taylor series expansion,

$$e^*(T) \approx e_0^* + \left(\frac{de^*}{dT}\right)_0 (T - T_0), \tag{A5}$$

where e_0^* and $(de^*/dT)_0$ indicate, respectively, the saturation specific humidity and its derivative with respect to temperature, evaluated at the reference temperature, T_0. The specific humidity difference between measurement height and snow surface is thus approximately,

$$q_a - q_s \approx \frac{0{\cdot}622}{p} RH_a \left[e_0^* + \left(\frac{de^*}{dT}\right)_0 (T_a - T_0)\right] - \frac{0{\cdot}622}{p} RH_s \left[e_0^* + \left(\frac{de^*}{dT}\right)_0 (T_s - T_0)\right]. \tag{A6}$$

It is convenient to linearize around the temperature that is used to define degree–days; that is, $T_0 = 0°C$. Now, for $T_a > T_0 = 0$,

$$\Delta Q \approx R_{net} + \rho C_h k^2 (\ln z/z_0)^{-2} u \Bigg\{ \overbrace{[(T_a - T_0) - (T_s - T_0)] C_p}^{\sim H} + \underbrace{\frac{L}{2} \frac{0{\cdot}622}{p} RH_a \left[e_0^* + \left(\frac{de^*}{dT}\right)_0 (T_a - T_0)\right] - \frac{L}{2} \frac{0{\cdot}622}{p} RH_s \left[e_0^* + \left(\frac{de^*}{dT}\right)_0 (T_s - T_0)\right]}_{\sim LE} \Bigg\}. \tag{A7}$$

Table AI. Physical constants used in estimating the restricted degree–day coefficient

Symbol	Physical constant	Value
m_Q	Energy to water depth conversion	0·026 cm W^{-1} m^2 day^{-1}
k	von Karman's constant	0·40
L	Latent heat of vaporization	2·5 × 106 J kg^{-1}
e_0	Reference vapour pressure	6·1 mbar
$\left(\frac{de^*}{dT}\right)_0$	Reference slope of vapour pressure on temperature	0·4438 mbar K^{-1} (at 0°C)

Equation (A7) represents a significant approximation early in the melt season when daily average snow surface temperature may fall well below zero, even though melt is occurring during part of the day.

It is reasonable to assume that the air at the snow surface is saturated with respect to water vapour, i.e., RH_s equals unity. Further assuming that the snow surface temperature is zero during the melting phase, Equation (A7) becomes,

$$\Delta Q \approx R_{net} + \rho C_h k^2 (\ln z/z_0)^{-2} u \left\{ \left[C_p + \frac{L}{2} RH_a \frac{0{\cdot}622}{p} \left(\frac{de^*}{dT}\right)_0 \right] T_d - (1 - RH_a) \frac{L}{2} \frac{0{\cdot}622}{p} \right\}. \tag{A8}$$

The term in brackets in Equation (A8) is divided and multiplied by T_d to obtain an equation for melt-water equivalent in the form

$$M = m_Q \Delta Q \approx m_Q R_{net} + a_r T \qquad [\text{cm day}^{-1}] \tag{A9a}$$

$$M \approx m_Q R_{net} + \underbrace{m_Q \rho C_h k^2 (\ln z/z_0)^{-2} u \left[C_p + RH_a \frac{L}{2} \frac{0{\cdot}622}{p} \left(\frac{de^*}{dT}\right)_0 - \frac{(1 - RH_a)}{T_d} \frac{L}{2} \frac{0{\cdot}622}{p} e_0^* \right]}_{a_r} T_d \tag{A9b}$$

which provides a mathematical expression to evaluate the restricted degree–day coefficient, a_r,

$$a_r \approx m_Q \rho C_h k^2 (\ln z/z_0)^{-2} u \left[\underbrace{C_p}_{\text{I}} + \underbrace{RH_a \frac{L}{2} \frac{0{\cdot}622}{p} \left(\frac{de^*}{dT}\right)_0}_{\text{II}} - \underbrace{\frac{(1 - RH_a)}{T_a} \frac{L}{2} \frac{0{\cdot}622}{p} e_0^*}_{\text{III}} \right] \tag{A10}$$

The wind speed, u, relative humidity, RH_a, and degree–day temperature T_d, are variable in time; representative values are selected. The turbulent transfer coefficient C_h is a function of T_d and u, and the remaining parameters may be treated as physical constants (Table AI).

Given time-series of all the constituent physical variables, a_r could, in principle, be estimated on a daily or even an hourly basis. However, if such detailed data were available, the modeller would be advised to use a full energy balance model, rather than the SRM. With a view to applications in data-sparse regions (and for climate change scenarios where general changes are more reasonably predicted than the future hour-to-hour variation of climate variables), this paper focuses on testing the RDD version of the SRM with a constant seasonal a_r.

Martinec (1989) assessed daily values of the restricted degree–day coefficient from measurements of lysimeter melt, net radiation and temperature at the Weissfluhjoch test site in the Swiss Alps; values of a_r generally ranged from 0·2 to 0·25 cm °C^{-1} day^{-1}. Using meteorological values typical of that location during the 1985 melt season (Table AII, column 3), an independent estimate of a seasonal a_r by Equation (A10) gives a value of 0·17 cm °C^{-1} day^{-1}, which lies slightly below the range of values found by Martinec (1989). When humidity (RH_a) is low, terms II and III in Equation (10) reduce a_r; in addition, a_r is directly proportional to wind speed (u). These functional dependencies are consistent with Martinec's (1989) observation of lower values on days with little wind and low air humidity.

Table AII. Estimation of the restricted degree–day coefficient

Characteristic physical quantity	Units	Weissfluhjoch 1985*	Sleepers river W-3 1969–1974† 1 March–30 June
$\ln^2(z/z_0)$‡		68·8	68·8
T_a	°C	3	5
p	mbar	750	950
ρ§	$kg\,m^{-3}$	0·95	0·98
U	$m\,s^{-1}$	3	3·5
RH_a		0·83	0·6
Results [Equation (A10)]			
Term I	$cm\,day^{-1}\,°C^{-1}$	0·17	0·25
Term II		0·06	0·05
Term III		−0·06	−0·10
a_r		0·17	0·20

* Average values from Kustas *et al.* (1994)
† Data from Anderson *et al.* (1977)
‡ $z/z_0 = (2\,m)/(0{\cdot}0005\,m)$ (measurement height)/(roughness length for snow)
§ $\rho = p/R_d T_a$, where R_d is the gas constant for dry air

Table AII (column 4) also shows the values used in computing the restricted degree–day coefficient for the Sleepers River Research Watershed W-3 for the simulation years of this study. From this analysis, a_r is assigned a fixed value of $0{\cdot}20\,cm\,°C\,day^{-1}$ throughout the season for all six years of the study.